Biophysical Chemistry, 48 (1993) 31–38
Elsevier Science Publishers B.V., Amsterdam

BIOCHE 01782

A new front-face optical cell for measuring weak fluorescent emissions with time resolution in the picosecond time scale

Zygmunt Gryczynski and Enrico Bucci *

Department of Biochemistry, University of Maryland at Baltimore, 108 North Greene Street, Baltimore, MD 21201 (USA)

(Received 24 March 1993; accepted 21 May 1993)

Abstract

Recent developments of ultrafast fluorimeters allow measuring time-resolved fluorescence on the picosecond time scale. This implies one is able to monitor lifetimes and anisotropy decays of highly quenched systems and of systems that contain fluorophores having lifetimes in the subnanosecond range; both systems that emit weak signals. The combination of weak signals and very short lifetimes makes the measurements prone to distortions which are negligible in standard fluorescence experiments. To cope with these difficulties, we have designed a new optical cell for front-face optics which offers to the excitation beam a horizontal free liquid surface in the absence of interactions with optical windows. The new cell has been tested with probes of known lifetimes and anisotropies. It proved very useful in detecting tryptophan fluorescence in hemoglobin. If only diluted samples are available, which cannot be used in front-face optics, regular square geometry can still be utilized by inserting light absorbers into a cuvette of 1 cm path length.

Keywords: Time-resolved fluorescence; Highly quenched systems; Front-face optics; Optical cell; New cuvette

1. Introduction

In the last decade, the use of cavity-dumped synchronously pumped dye-lasers [1] has allowed the construction of time-correlated instruments with an impulse response of 20 ps band width, and of frequency-domain apparatus with resolution up to 10 GHz [2–4]. This paved the way to the investigation of fluorescent systems with very short lifetimes, in the picosecond range, usually associated with very low emission intensity.

This type of analysis can give important information on conformational states of proteins and nucleic acids, protein–protein, protein–membrane and protein–nucleic acids interactions, and on internal dynamics of proteins, peptides and amino-acids residues [5–9]. In particular, investigation of the heavily quenched emission of tryptophan from heme-containing proteins, appears to be a powerful tool for exploring ligand linked conformational changes [10–14].

The combination of low intensity and short lifetimes makes these measurements sensitive to artifacts that are insignificant in standard (classic) fluorescence experiments. Therefore, we have de-

* Corresponding author.

signed a new optical cell (here indicated as GB cell, which stands for Gryczynski–Bucci cell [1]), and have standardized procedures, which allow precise measurements of lifetimes by front-face techniques. This technique requires high concentrations of the fluorophores to be investigated, which often is not possible for biological samples. For this reason, we have also standardized measurements in classic square geometry, using cuvettes of 1 cm path length, internally shielded from unwanted reflections.

2. Relevant artifacts in measuring picosecond lifetimes

2.1. Purity of the samples

Purity is important when heavily quenched systems are used. Typical examples are hemoproteins where the emission of tryptophan is quenched between 50 and 100 times by energy transfer to the heme [15], which results in lifetimes of 10–30 ps. This implies that a 1% component with a lifetime of 2 ns (as for non-quenched tryptophan) will produce 40% of the total emission intensity. A 3–5% impurity will practically obscure the emission of the sample.

2.2. Optical distortions

The speed of light becomes a relevant instrumental parameter when the investigation of time-resolved fluorescence extends to the nanosecond and subnanosecond time scale. In fact, ultrafast technology is based on time comparisons between the excitation (reference) and emission beams. Therefore, it is important that the beams *per se* are synchronous, so as to produce coherent images on the photodetector, and that they travel identical optical distances in the fluorimeter between the sample and the photodetector.

[1] A brief schematic description of the GB cell hes been reported in ref. [14].

2.2.1. Desynchronization of the beams

Laser light is synchronous (coherent) at the origin, however, the optical components of the instrument can produce desynchronization of the beams. Using square geometry and a 1 cm cuvette, the incident beam takes 50 ps to pass from one face of the cuvette to the other. This implies an identical time spread for the excitation, not necessarily matched by identical spread of the emission. Also, the light emitted from a 1 cm front and focused on the photodetector, travels different distances depending on whether it originates from the edges or from the center of the cuvette. It can be estimated that, if the cuvette is at 10 cm from the focusing lens, the two paths differ by 0.3 mm, i.e. 2 ps for the light beams. Finally, if the emitted light is very weak, monochromators and filters will be used for selecting the emission wavelength with broad band-widths of 30–35 nm or more. The red and blue parts of the filtered light have different speed and will contribute to the desynchronization of the emitted beam. Other difficulties contribute to distort the synchronization of the beams, like color effects of the detector and secondary processes (reflections) in interference filters and monochromators.

Desynchronization distorts the shape of the impulse response in time-correlated instruments. In the frequency domain, it increases the demodulation making it inconsistent with the phase shift. Clearly, the square cuvette must have the shortest possible path and filter band widths should be as narrow as possible. With front-face techniques, it is possible to use high optical density samples, which prevents penetration of the excitation beam, thereby, eliminating the distortions produced by the geometry of a square cuvette. Furthermore, the higher intensity of the signal allows shorter band widths.

2.2.2. The optical distance

In the optical path, both excitation and emission beams have to pass through lenses, filters, polarizers, and the emission window of the sample cuvette and the window of the photodetector. It can be estimated that the total widths of these components is about 50 mm of quartz. In trypto-

phan fluorescence, for the excitation beam at 290 nm (refraction index $n = 1.49$), the time necessary to travel through the quartz panes can be estimated to be near 249 ps. For the emission beam at 350 nm ($n = 1.47$) the time is 253 ps thus, the excitation beam has a delay of 4 ps.

In time domain, this difficulty is partially resolved by numerically shifting the position of the impulse response in the analysis of the decay data.

In frequency domain, the optical distances of the reference and emission beams must be calibrated. This can be accomplished by observing the phase of light scattered from the sample compartment with the same wavelength of the excitation and emission beams, respectively. The observation is performed in the presence and absence of the respective filters, polarizers, and lenses monitoring the phase shift that these components produce in the respective beam. The two shifts can be equalized by inserting additional quartz plates or neutral density filters in the optical paths. For tryptophan fluorescence, we have successfully used the doubled beams of a rhodamine laser at 295 nm and of a pyridine-2 dye lasers at 345 nm, scattered from an aluminum plate. We were able to equalize travel time along the optical path to within ± 1 ps. A residual error is still present because it is not possible to eliminate the windows of the sample cell and of the photodetector when the calibration is performed. Thin cell windows are recommended.

3. Current use of front-face techniques

One of the main problems connected with low intensity emission is the Raman scattering from water. Figure 1 shows the emission spectrum of a hemoglobin solution measured in square geometry optics with a 1 cm cuvette. Evidently, the spectrum is dominated by the Raman scattering which totally obscure the emission from hemoglobin. The best way for eliminating the Raman scattering is to use front-face techniques. In this technique, the high optical density of the solution allows a very short penetration of the exciting light, thereby decreasing the scattering

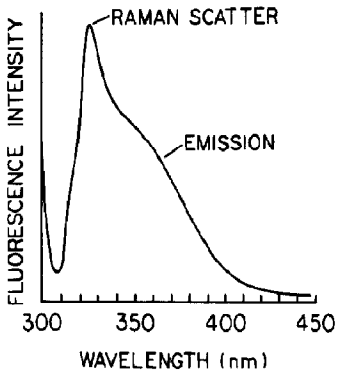

Fig. 1. Fluorescence emission spectrum of human oxy-hemoglobin in 0.03 M phosphate buffer at pH 7.0 in a cuvette of 1 cm path length, right angle geometry. Excitation was at 295 nm. Protein concentration 3 μM.

from the solution. Also, the Raman scattering is proportional to the fourth power of the sine of the angle between the excitation beam and the direction of the observation. Therefore, it has a maximum value for a 90° angle and it falls very rapidly for lower angles. Front-face techniques allow substantial lowering of the angle, at 34° the intensity of the Raman scattering is decreased 10 times.

It is also very important to note that surface phenomena at the interface between the solution and the quartz window may denature proteins and other biomolecules, and that the high energy of the incident laser beam contributes to the denaturation. Front-face technology is used with solutions of high optical density, so as to prevent penetration of the excitation light. Therefore, the emission is produced by the most superficial layers of the solutions, where the surface denaturation is maximal. This may produce severe distortions of the data.

Eisinger and Flores [16], describe an adaptation of front-face technique to commercial square geometry instruments by tilting the cuvette in the sample compartment at 34° with respect to the excitation beam. The angle between excitation and emission is still 90°, allowing a maximum value for the residual Raman scattering. Also, in the tilted cuvette, neither the excitation nor the emitted beams are oriented perpendicularly to the quartz windows, therefore, the different re-

fractive index for vertical and horizontal polarized light modifies the relative polarization of the beams, introducing distortions in anisotropy measurements. These distortions apply, also, to the value of the magic angle of polarized light, used for eliminating the rotational diffusion components in the emission.

Horiuchi and Asai [17], have designed a square cuvette with thick windows where the inside compartment is tilted, while the outside walls are still in a square position. This eliminates most of the difficulties with polarization, because, both excitation and emission beams are oriented perpendicularly to the external faces of the windows. However, it introduces in the optical path, the additional thickness of the cuvette and leaves the residual Raman scattering to its maximum value.

Both the techniques proposed by Eisinger and Flores [16] and Horiuchi and Asai [17] cannot avoid problems connected with surface denaturations at the liquid–quartz interface.

4. The GB cell

Figure 2 shows a schematic of the cuvette that we designed. It is essentially a conical cup which presents to the excitation beam a horizontal liquid surface free of interactions with quartz windows. A cover slides over the cuvette, through which both the excitation and emission beams are channelled, to avoid spilling reflections. The emission channel is centered on the normal to the liquid surface and the excitation channel makes a 34° angle with it. The emission channel has a conical shape that helps in sending reflections either away from the observation, or to be trapped by additional diaphragms positioned in top of the channel. If it is necessary to equilibrate samples with special gas mixtures, quartz windows can be inserted at the top of the emission and excitation channels, as well as the necessary vents, on the cover of the cuvette. At the bottom of the cuvette there are two additional windows for allowing absorption measurements. One of these windows is mounted on a sliding sleeve, for adjusting the optical path and for regulating the height of the liquid level in the cell. The proper direction of the excitation and emission beams are obtained using metallic mirrors, chosen for minimal distortions of the polarization of the light. Cooling jackets can be used for thermostating the samples.

It should be stressed that even if windows are positioned on top of the two channels, the liquid surface of the sample is not in contact with window panes, therefore, no denaturation occurs at the contact between the sample and the windows.

The 34° angle between emission and excitation decreases about tenfold the intensity of the resid-

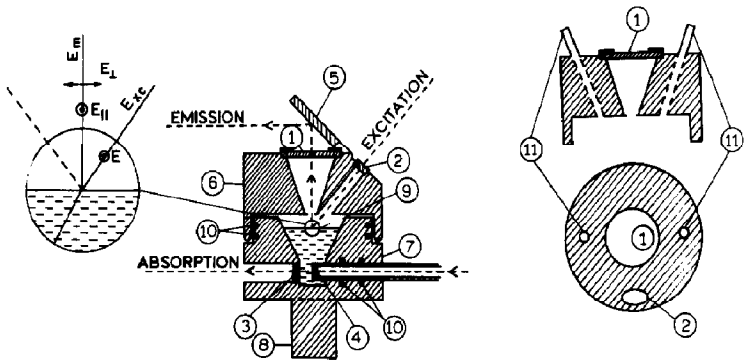

Fig. 2. Schematics of the GB cell: (1) emission channel, (2) excitation channel, (3) fixed window, (4) sliding window, (5) metallic mirror, (6) cover of the cuvette, (7) body of the cuvette, (8) supporting stem, (9) liquid surface, and 10) "O" rings.

ual Raman scattering. Also, both excitation and emission are perpendicular to the optional windows in the excitation and emission channels, thereby, eliminating distortions in anisotropy measurements. When anisotropy is measured, the excitation beam must be polarized with the electric vector parallel to the surface of the liquid, and perpendicular to the plane described by excitation and emission beams. On this configuration, the magic angle can be obtained by rotating the polarizer in emission to 36°.

Figure 3 shows a comparison of the impulse response obtained in time domain using ludox solutions in front-face in the GB cell, and in square geometry in a 1 cm cuvette. In the GB cell, the optical density of the solution was increased to about 20 OD units/cm by additions of crystalline hemin chloride. The figure shows that the impulse response had a band width of 23 ps for the front-face cuvette and of 28 ps for the square cuvette. This difference was probably due to the more coherent image produced by the front-face measurements and to the total absence of reflections in the GB cell. The shape of the impulse response shows the presence of reflections (indicated with 1 and 2) in square geometry, while in front-face, there was only the usual after pulse of the photomultiplier. When the heme was omitted from the ludox solution in the GB cell, so as to allow a maximum penetration producing reflections and Raman scattering, the shape of the impulse response did not change and its band width increased to 25 ps. The decay of the impulse response still did not show detectable reflections.

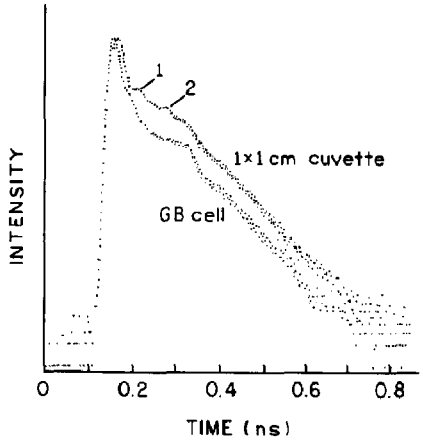

Fig. 3. Impulse response from a ludox solution in a 1 cm path length square cuvette (upper curve) and in the GB cell. In the GB cell hemin chloride was added up to 20 OD units/cm. Arrows 1 and 2 show major reflections generated in the square cuvette. The doubled beam of a rhodamine laser at 295 nm was used in excitation.

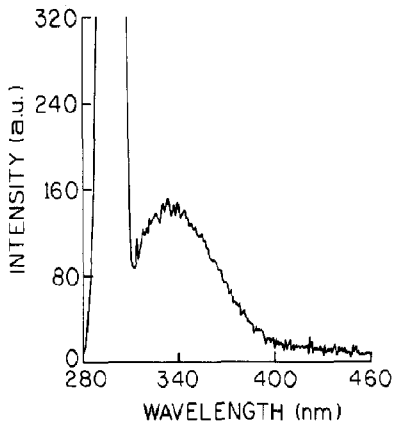

Fig. 4. Emission spectrum of human oxy-hemoglobin in 0.03 *M* phosphate buffer at pH 7.0 in the GB cell, front-face geometry. Excitation was at 295 nm. Protein concentration 0.4 m*M*.

Figure 4 shows the emission spectrum obtained from a 0.4 m*M* solution of hemoglobin in the GB cell. Excitation was at 295 nm from a frequency-doubled rhodamine dye-laser and after the scattering of the excitation beam, the figure shows the spectrum of tryptophan with emission maximum around 332 nm. The Raman scattering present in Fig. 1 is practically eliminated. Other fluorophores have been tested in the GB cell (e.g. DPH [2], DPO [2], tryptophane) and their emission spectra matched those expected from classic fluorescence [18].

Figure 5 shows the frequency dependence of the phase-shift and demodulation of DBS [2] which is known to have a single lifetime in the picosecond range [19]. The measurements, performed at 20°C and 45°C, gave single exponential decays with lifetimes of 185 and 102 ps, respectively. We

[2] Abbreviations used: DBS = 4-Br,4-dimethylamino stilbene; DPH = 1,6-diphenylhexatriene; and DPO = 1,8-diphenyloctatetraene.

also tested the GB cell for the presence of distortions in emission anisotropy measurements. As expected, a solution of pyrene at high concentration in cyclohexane showed no anisotropy when the emission of the excimer was monitored at 510 nm. We also examined the emission anisotropy of DPH, DPO, and Dioxido-*p*-terphenyl in stretched films of polyvinyl alcohol as a function of measured dichroic ratio, R_d, so as to make emission anisotropy independent of stretched procedure [21]. The films were cut in disks, which were positioned inside the conical cup of the GB cell, with the stretching direction parallel to the polarization of the excitation. These anisotropies have been studied in detail [20–22] and it was found that for a wide range of anisotropy (−0.3 to +0.9), our data corresponded very well to those of the literature. Also, we compared the polarization of tryptophan in glycerol at −5°C both in square geometry and in the GB cell. Figure 6 shows that there was a perfect correspondence between the two sets of data.

These data prove that the GB cell system, including the metallic mirror, does not distort lifetimes and anisotropy signals. Thus, the GB cell appears to resolve practically all of the difficulties mentioned in the introduction, for measuring time-resolved fluorescence in the picosecond range.

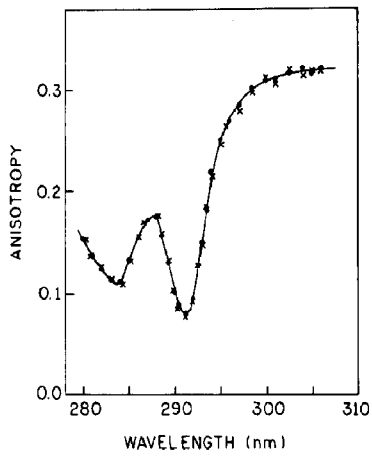

Fig. 6. Steady state excitation polarization spectrum of tryptophan in glycerol at −5°C. (●) Square geometry (×) GB cell. Emission monitored at 340 nm. The continued line is hand-drawn through the points.

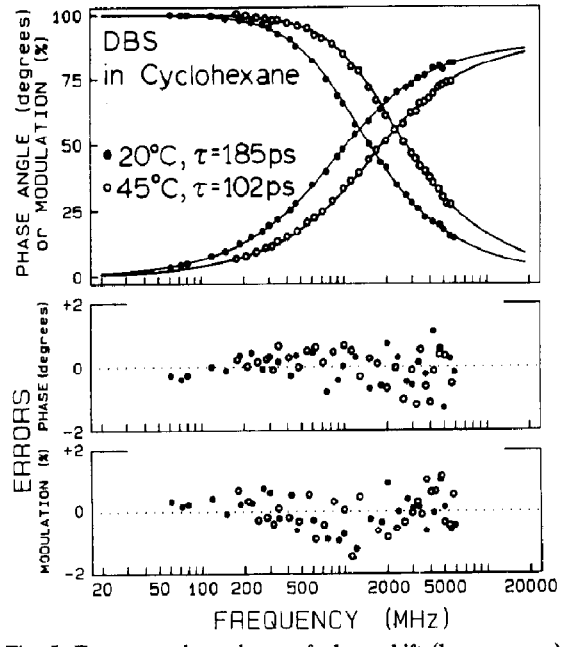

Fig. 5. Frequency dependence of phase shift (lower curves) and demodulation (upper curves) of DBS in cyclohexane, in the GB cell. The lower panels show the respective distribution of errors between experimental and computed data.

5. The "shielded" cuvette, an alternative to the "Holtom" cuvette

The "Holtom" cuvette is 3 mm square cell having two black windows: one opposite to the excitation beam for absorbing the excitation light after passage through the solution, and the other opposite to the photodetector for absorbing the back reflections of the emitted light [4]. With this cuvette, it is possible to obtain a 24 ps bandwidth impulse response in time domain. These distortions are very small and can be tolerated in most experiments. The cuvette is very useful for biological samples, for which the high concentrations necessary for front-face geometry is not available. However, when biological samples are used, it is often advantageous to measure optical absorptions in the same cuvette used for fluorescence experiments. Furthermore, it may be necessary to stir the contents of the cuvette. In these cases, we use a 1 cm square cuvette masked as shown in Fig. 7, so as to observe the emission from a very

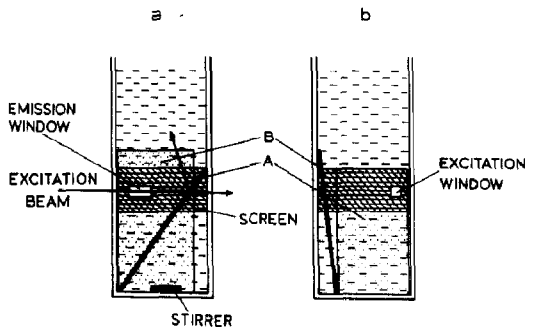

Fig. 7. The "shielded" cuvette. The cuvette is shown from the emission (a) and excitation side (b). Two slanted neutral density filters are inserted as indicated for absorbing the residual excitation light and the back reflection at fluorescence of the sample. The two sides are masked with black Kodak paper. In excitation, the 1 mm^2 window is positioned at 1 to 2 mm from the side of the cuvette. In emission, the 2×3 mm window can be positioned at any desired distance from the side of the cuvette, depending on the optical density of the sample, which allows more or less penetration of the excitation light.

small region of the cuvette. In place of the black windows, as in the "Holtom" cuvette, we use, in the same positions, two neutral density filters with OD near 1.0. The filters are cut from commercially available $2'' \times 2''$ filters. They are positioned in a slanted way, as shown in Fig. 7, so as to absorb reflections and send what is left toward the top of the cuvette. The inserted filters leave a space at the bottom of the cell for a small magnetic stirrer, and the optical absorption of the solution can be observed through the sample above the filters. Experiments with ludox solutions indicate a very similar behavior of this "shielded" cuvette and of the "Holtom" cuvette. In frequency-domain, the "shielded" cuvette has been used for measuring the lifetime of several probes with single lifetimes in the picosecond range [19]. When DBS solutions were used results very similar to those shown in Fig. 5 were obtained.

6. Conclusions

The possibility of measuring time-dependent lifetimes and anisotropy in the picosecond range, promises a wealth of information regarding the excited state of fluorophores, and will shed new light on the study of macromolecules and their interactions. These measurements are subject to a series of potential artifacts, negligible in classic fluorescence experiments. These problems, however, appear to be largely resolved both in front-face and square geometry optics by the use of the GB cell, the "Holtom" cuvette, and the "shielded" cuvette.

Acknowledgments

This work was supported in part by NIH PHS Grants HL 13164 (E.B.) and HL 33629 (E.B.) by the Center for Fluorescence Spectroscopy at the University of Maryland at Baltimore Grants NIH-GM-39G17 and NSF-DIR-8710401, by the Regional Laser Laboratory at the University of Pennsylvania Grant NIH-RR01348 and by the Laboratory for Fluorescence Dynamics at the University of Illinois at Urbana Grant NIH-RR03155.

References

1 R.F. Steiner, G. Holtom and Y. Kubota, Laser spectroscopy of nucleic acid complexes, in: Lasers in Polymer Science and Technology: Applications 4 eds. J.P. Fouassier and J.F. Rabele (CRC Press, Boca Raton 1989).
2 G. Laczko, I. Gryczynski, Z. Gryczynski, W. Wiczk, H. Malak and J.R. Lakowicz, Sci. Instrum. 61 (1990) 2331–2337.
3 B. Barbieni, F. De Piccoli, M. van de Ven and E. Gratton, Time-resolved laser spectroscopy in biochemistry II, SPIE 1204 (SPIE, Bellingham, WA, 1990) pp. 158–170.
4 G.R. Holtom, Time-Resolved Laser Spectroscopy in Biochemistry II, SPIE 1204 (SPIE, Bellingham, WA, 1990) pp. 2–12.
5 D.M. Jameson and G.D. Reinhart (eds.), Fluorescence Biomolecules. Methodologies and Applications (Plenum Press, New York, 1986).
6 G.R. Fleming, Chemical applications of ultrafast spectroscopy (University Press, New York, 1986).
7 A.P. Demchenko, Ultraviolet spectroscopy of proteins (Springer, Heidelberg, 1986).
8 J.R. Lakowicz (ed.), Time-resolved spectroscopy in biochemistry II and III, SPIE 1204 (SPIE, Bellingham, WA, 1990).
9 J.R. Lakowicz (ed.), Topics in Fluorescence Spectroscopy, Vols. 1–3 (Plenum Press, New York, 1991).

10 G. Weber and F.W.J. Teale, Disc. Faraday Soc. 27 (1959) 134–141.
11 B. Alpert, D.M. Jameson and G. Weber, Photochem. Photobiol. 31 (1980) 1–4.
12 A.G. Szabo, D. Krajcarski, M. Zukes, and B. Alpert, Chem. Phys. Lett. 108 (1984) 145–149.
13 E. Bucci, H. Malak, C. Fronticelli, I. Gryczynski, G. Laczko, J.R. Lakowicz, Biophys. Chem. 32 (1988) 187–198.
14 E. Bucci, Z. Gryczynski, c. Fronticelli, I. Gryczynski and J.R. Lakowicz, J. Fluorescence 2 (1992) 29–36.
15 Z. Gryczynski, E. Bucci and T. Tenenholtz, Biophys. J. 63 (1992) 648–653.
16 J. Eisinger and J. Flores, Anal. Biochem. 94 (1979) 15–21.
17 K. Horiuchi and H. Asai, Biochem. Bioph. Res. Com. 97 (1980) 811–818.
18 J.B. Berlman, Handbook of fluorescence spectra of aromatic molecules (Academic Press, New York, 1971).
19 J.R. Lakowicz, I. Gryczynski, G. Laczko and D. Gloyna, J. Fluorescence 1 (1991) 87–93.
20 A. Kawski and Z. Gryczynski, Z. Naturforsch. 41a (1986) 1195–1199.
21 Z. Gryczynski and A. Kawski, Z. Naturforsch. 42a (1987) 1396–1398.
22 Z. Gryczynski and A. Kawski, Z. Naturforsch. 43a (1988) 193–195.